SHUNT ACTIVE POWER CONTROL BASED ON FEED-FORWARD NEURAL NETWORK.

Gideon F.Tano-Boamah [1]

Department of Electrical/Electronic Engineering, Kwame Nkrumah University of Science and Technology.

Keywords: Feed-Forward Neural Network, Harmonics Compensation, Shunt Active Power Filter, Frequency, Power Quality, Total Harmonic Distortion, Power factor.

ABSTRACT: *The shunt active power filter (SAPF) represents a prevalent instrument for the mitigation of harmonic distortions in three-phase electrical power systems. Numerous control methodologies have been established, encompassing approaches grounded in Artificial Neural Networks. Nevertheless, the conventional feedforward neural network, which has demonstrated efficacy in addressing various nonlinear challenges, has yet to be utilized with optimal performance in the execution of the SAPF control aimed at producing the reference currents for three-phase inverters. To validate the potential of this straightforward neural architecture, this study delineates an appropriate application strategy, predicated on the precise estimation of the Fourier coefficients associated with the fundamental harmonic of any distorted voltage or current. The aims included harmonic reduction and enhancement of the power factor. By utilizing simulations and experimental design, we evaluated practical scenarios, thereby confirming the feasibility of the recommended strategy.*

1. INTRODUCTION

Power systems, particularly distribution networks, are facing significant challenges related to power quality in the current era of advanced power electronics [26,11,16]. The expansion of power electronics-based nonlinear loads is causing harmonics within distribution systems. The widespread deployment of such nonlinear equipment has escalated the need for harmonics mitigation and reactive power compensation [27].

The adverse effects of poor power quality, resulting from the presence of harmonics and distortions, include power loss, resonance, overheating, and failures of power protection devices and electrical and electronic equipment. These issues impose substantial costs on both consumers and utility providers[28, 18, 9]. Addressing power quality concerns necessitates dedicated attention and extensive efforts for improvement. Harmonics generated by nonlinear loads induce voltage distortion, adversely affecting other connected loads at the same point of common coupling. Researchers over the years various methods for mitigating the harmonics in the power system. Initially, capacitor banks were suggested as a solution which were found to be ineffective in periods of overvoltage. Also, the issue of resonance arises when the reactance offered by the capacitor bank becomes equal to the system inductive reactance.[29] In that event, filters were developed to address harmonics and reactive power issues in power systems. Several traditional methods including Instantaneous Active Power and Reactive Power Theory, and Synchronous Reference Frame Theory have been used in controlling the SAPF to detect and mitigate harmonics. The traditional methods employ the use of filters which limit their ability to handle non-linear and timevarying characteristics of the system. Other traditional methods used in SAPF that are PI controllers and Repetitive controllers perform poorly in unbalanced and non-ideal cases. The advent of machine learning techniques has brought new opportunities for controlling SAPFs resulting in more efficient and accurate power quality enhancement[12, 18, 21]. Artificial Intelligence (AI) based control methods such as Artificial Neural Networks have shown great potential in enhancing the performance of SAPFs and can learn from

system behavior and adapt to changing operating conditions which traditional techniques cannot do. The AI based technique control can improve the accuracy and speed of the system and can handle complex non-linear system.
In retrospect of the ongoing research in the application of AI techniques in controlling the Shunt Active Power Filter, we aim to design a SAPF controller based on AI techniques.

2. METHOD OF COMPENSATION

The Fourier Transform is a mathematical operation that transforms a time-domain function f(t) into a frequency-domain representation $F(\omega)$, where ω represents angular frequency.

This transformation expresses the original function as a sum of sinusoids with varying amplitudes and phases. With the frequency domain analysis, signals are decomposed as the sum of fundamental $\sin\omega t$ and $\cos\omega t$ with harmonics.

$$F(\omega) = \int_{-\infty}^{\infty} f(t) e^{-i\omega t} dt \tag{0}$$

Where:

- $F(\omega)$ is the Fourier Transform of f(t)

However three-phase quantities of periodic due to their sinusoidal nature. The transformation of continuous of periodic signals leads to the formation of Fourier Series.

The Neural network is the control system of the proposed shunt active power filter. For the neural network to actively provide accurate reference current for the power converter, the data of the system must be fed to the control block. Because the voltage and current of a three-phase system are continuous time signals there is a need to convert these waveforms into discrete waveforms. Sampling is done by multiplying the continuous signal by a delta function or an impulse train. The neural networks are designed to process discrete signals. Fourier transforms are used in the generating of reference current. The computation of Fourier transforms of continuous signals is complex. Sampling produces periodic and finite signals.[1]

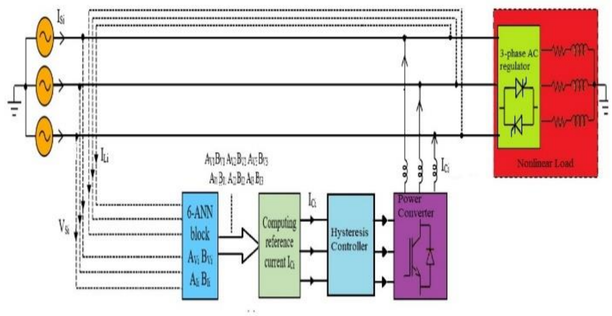

Figure 1. A general of overview of the proposed system into the transformer-less grid

The distorted current waveform can be described as the combination of various sinusoidal components, each with frequencies that are multiples of a base frequency.[1]

$$I_{L,i}(t) = \sqrt{2}\, I_{I,i}\cos(\omega t - \varphi_{1.i}) + \sqrt{2} \sum_{\forall h\geq 2} I_{h,i} \cos(h\omega t - \varphi_{h,i}) \tag{1}$$

$$I_{C,i}(t) = I_{L,i}(t) - I_{S,i}(t) = \sqrt{2} \sum_{\forall h\geq 2} I_{h,i} \cos(h\omega t - \varphi_{h,i}) \tag{2}$$

The source current obtained after compensation is

$$I_{S,i}(t) = \sqrt{2}\, I_{I,i}(\cos(\omega t - \varphi_{1.i}) \tag{3}$$

Which is expressed through their rectangular components as,

$$I_{S,i}(t) = \sqrt{2}\, I_{I,i}\cos(\omega t - \varphi_{1.i}) = \sqrt{2}\, I_{I,i}\cos\varphi_{1,i}\cos\omega t + \sqrt{2}\, I_{I,i}\sin\varphi_{1,i}\sin\omega t = A_{I,i}\cos\omega t + B_{I,i}\sin\omega t \quad (4)$$

Where $A_{I,i}$ and $B_{I,i}$ are real numbers representing the rectangular coefficients of the fundamental source current. Which imply the compensation current obtained is expressed as

$$I_{C,i}(t) = I_{L,i}(t) - (A_{I,i}\cos\omega t + B_{I,i}\sin\omega t) \quad (5)$$

The expressions for the compensating currents of the 3-phases:

$$I_{C,a}(t) = I_{L,a}(t) - (A_{I,i}\cos\omega t + B_{I,i}\sin\omega t) \quad (6)$$

$$I_{C,b}(t) = I_{L,b}(t) - (A_{I,i}\cos(\omega t + 2\pi/3) + B_{I,i}\sin(\omega t + 2\pi/3)) \quad (7)$$

$$I_{C,c}(t) = I_{L,c}(t) - (A_{I,i}\cos(\omega t - 2\pi/3) + B_{I,i}\sin(\omega t - 2\pi/3)) \quad (8)$$

3. POWER FACTOR COMPENSATION

The APF is designed to inject currents aimed at reducing harmonic distortion and correcting the power factor. Power factor correction is achieved when the source current, following compensation, aligns closely with the voltage phase. To ensure this alignment, a corrective factor derived from the phase voltages is used. These corrective factors help adjust the compensation currents so that the phase currents are nearly in phase with the voltages. This correction is essential because current distortion leads to corresponding voltage distortion.[1]

$$I_{S,i}(t) = G\, V_{S,x}(t) \quad (9)$$

Where G is the corrective factor or equivalent conductance

$$G = \frac{P}{V^2} = \frac{P}{V_a^2 + V_b^2 + V_c^2} \quad (10)$$

P represents the average power used by the load, while V is the RMS value of the three-phase voltage, calculated from the RMS values of the phase voltages. The phase voltages are displaced by 120 degrees from each other, and the source voltage is:

$V_{S,x}(t) = \sqrt{2}\, V_{S,x}\cos(\omega t + \alpha)$ where α is the displacement angle.

The FFNN could also generate a rectangular coefficient of the voltage as:

$$V_{C,a}(t) = V_{L,a}(t) - (A_{V,a}\cos\omega t + B_{V,a}\sin\omega t) \quad (11)$$

$$V_{C,b}(t) = V_{L,b}(t) - (A_{V,b}\cos(\omega t + 2\pi/3) + B_{V,b}\sin(\omega t + 2\pi/3)) \quad (12)$$

$$V_{C,c}(t) = V_{L,c}(t) - (A_{V,c}\cos(\omega t - 2\pi/3) + B_{V,c}\sin(\omega t - 2\pi/3)) \quad (13)$$

$$P_i(t) = V_i(t) \cdot I_i(t) = (A_{V,i}\cos\omega t + B_{V,i}\sin\omega t) \cdot (A_{I,i}\cos\omega t + B_{I,i}\sin\omega t)$$

(14)

I = a,b,c. The application of some trigonometric identities (14) allow us to obtain eqn (15)

$$: \ P_i(t) = A_{V,i}A_{I,i} + \frac{A_{V,i}B_{I,I} + B_{V,i}A_{I,i}}{2} \cdot \sin 2\omega t + (B_{V,i}B_{I,i} - A_{V,i}A_{I,i})\sin^2\omega t$$

(15)

The active power for the phase current I is the average value of $P_i(t)$ over a period. This is:

$$P_i = \frac{1}{T}\int_0^T P_i(t)dt = \frac{A_{V,i}A_{I,i} + B_{V,i}B_{I,i}}{2}$$

(16)

In a three-phase system, the calculation of the three active powers of each phase (17) determines the total active power:

$$P_i = \frac{1}{2}(A_{V,a}A_{I,a} + B_{V,a}B_{I,a} + A_{V,b}A_{I,b} + B_{V,b}B_{I,b} + A_{V,c}A_{I,c} + B_{V,c}B_{I,c})$$

(17)

The rms value of the three-phase voltage as a function of rectangular coefficients, therefore:

$$V^2 = V_a^2 + V_b^2 + V_c^2$$

(18)

Where for each of the phases it is verified as :

$$\sqrt{2}\ Vi = \sqrt{Avi^2 + Bvi^2}$$

(19)

And therefore :

$$V^2 = \frac{1}{2}(A_{Va}^2 + B_{Va}^2 + A_{Vb}^2 + B_{Vb}^2 + A_{Vc}^2 + B_{Vc}^2)$$

(20)

From (17) and (20), G is obtained as:

$$G = \frac{A_{Va}A_{Ia} + B_{Va}B_{Ia} + A_{Vb}A_{I} + B_{Vb}B_{Ib} + A_{Vc}A_{Ic} + B_{Vc}B_{Ic}}{A_{Va}^2 + B_{Va}^2 + A_{Vb}^2 + B_{Vb}^2 + A_{Vc}^2 + B_{Vc}^2}$$

(21)

The conductance equivalence factor G expressed in simple terms of the rectangular coefficients as:

$$G = \frac{A_V A_I + B_V B_I}{A_V^2 + B_V^2}$$

(22)

$$I_{C,i}(t) = I_{L,i}(t) - GV_{s,i}$$

(23)

$$I_{C,a}(t) = I_{L,a}(t) - G(A_V\cos\omega t + B_V\sin\omega t)$$

(24)

$$I_{C,b}(t) = I_{L,b}(t) - G(A_V\cos(\omega t - 2\pi/3) + B_V\sin(\omega t - 2\pi/3))$$

(25)

$$I_{C,c}(t) = I_{L,c}(t) - G(A_V\cos(\omega t + 2\pi/3) + B_V\sin(\omega t + 2\pi/3))$$

(26)

The Fourier coefficients are used to reconstruct the source current into continuous form using:

$$a0 + \sum_{n=1}^{\infty}\left(\text{ancos}\left(\frac{2\pi nx}{T}\right) + bnsin\left(\frac{2\pi nx}{T}\right)\right)$$

(27)

4. ARTIFICIAL NEURAL NETWORK

The feed-forward neural network consists of a determined number of neurons, organized in two or more layers, highly interconnected. The neuron operation consists of applying a determined transfer function to a weighted sum of its inputs. It is usual the choice of a “tan-sigmoid” transfer function for hidden layers and a “linear” function for output layer. The performance index, MSE measures the accuracy of the neural network.[1]

$$mse = \frac{1}{m}\sum_{i=1}^{m}||y-t||^2 \quad (27)$$

where m = number of training patterns and y and t corresponding to output and target vectors respectively. The backpropagation algorithm uses the mean square error to re-adjust the interconnection weights to reduce the mean square error. This cycle is iteratively repeated until the mean square error reaches a small enough value. In this project, different backpropagation training algorithms were used such as Bayesian Regulation, Scaled Conjugate Gradient, resilient backpropagation, and Levenberg-Marquardt algorithm. Among them, the Levenberg-Marquardt algorithm gave the best mean square error which is 6.7 x 10^{-6} with less number of epochs about 11 epochs. The resilient backpropagation algorithm provided a similar mean square error but with more number of epochs about 35 epochs.

After a huge number of tests with different points per cycle and number of FFNN inputs, a slow sampling rate of 5 kHz could be chosen, with 30 points per waveform cycle, which means that the neural network must contain 30 inputs. For the strategy of extracting the fundamental harmonic, there was no need to increase the number of samples. It also works with faster sampling, but at the cost of increasing the size and complexity of the FFNN, as well as the training times, without achieving higher performance.
Different harmonic spectrums of nonlinear loads were analyzed to choose suitable magnitudes of the different harmonics. The control approach for the Shunt Active Filter involves sampling each waveform cycle of current or voltage to provide the input for the Artificial Neural Network. The method was initially tested at a standard 50 Hz frequency. We aimed at making the model function effectively across a range of frequencies. For the 50 Hz case, the ANN provides rectangular coefficients for the fundamental harmonic every 20 milliseconds. It is important for the control method to perform optimally even with variations from the standard 50 Hz. To ensure the model stability. The training data had multiple waveforms with frequencies that were close to the fundamental frequency. The training patterns incorporated frequencies varying between 49.5 and 50.5 Hz.[1]

A voltage source inverter was used as a power conversion within the framework of the Shunt Active Power Filter (SAPF). The inverter facilitates the transformation of direct current (DC) voltage obtained from the DC link capacitor into alternating current (AC) outputs, which are subsequently integrated into the electrical power system. The DC link capacitor serves as the voltage source essential for the functionality of the inverter.[8, 9, 15, 25]

An Insulated gated bipolar transistor-based inverter is proposed because IGBTs combine the added advantages of MOSFET and BJT. The IGBTs act as switches in the inverter circuit. The gating signals for the IGBTs are generated by a current control technique.

5. SIMULATION

This project was simulated in MATLAB/Simulink environment. It demonstrated the application of artificial intelligence methods to control a shunt active power filter to mitigate harmonics generated by non-linear loads.
The systems parameters were as follows:

Table 1. A table of system parameters used in the simulation

PARAMETERS	VALUES
AC Source Voltage	415V
System Frequency	50Hz
Total line impedance per line	Rs =0.012 Ω, Ls = 0.0625 mH
Sampling Frequency	5000 Hz
Hysteresis controller	Hysteresis band ±0.07
SHUNT ACTIVE POWER FILTER	
Filter Impedance	Ls = 4.06 mH

DC Link Capacitor Voltage	415 V
DC Link Capacitor Capacitance	4700 μF
LOAD	
Resistance	20Ω
Inductance	90 mH

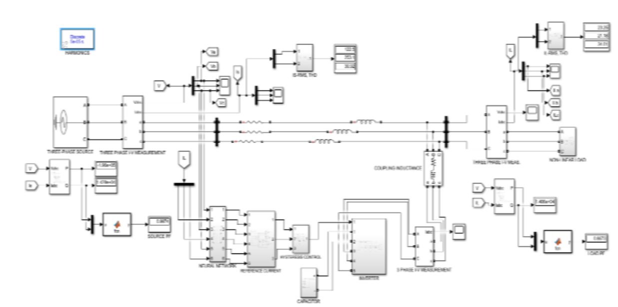

Figure 2. Simulation of the proposed system in MATLAB

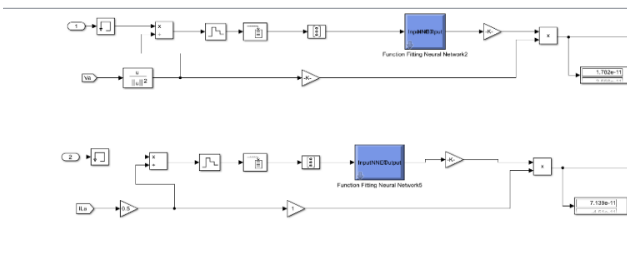

Figure 3. An illustration of the neural network controller of the SAPF

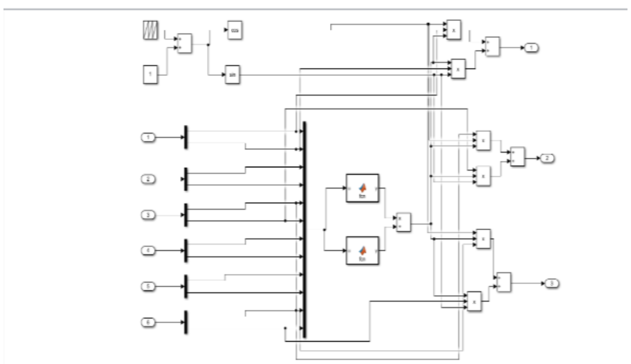

Figure 4. An illustration of the calculation of the source current

6. RESULTS AND ANALYSIS

This chapter presents the findings from the simulations along with a comprehensive analysis of the results. The main aim of minimizing harmonic distortion was evaluated by measuring the Total Harmonic Distortion (THD) of the system, with a target of achieving values below 5%. Additionally, the unity power factor compensation control method aims to attain a power factor close to one, alongside maintaining a low THD.

An unbalanced nonlinear load scenario arises when a diode bridge rectifier is linked to a three-phase unbalanced R-L load. The harmonic spectrum analysis for phase three, before any compensation, is presented. The total harmonic distortion of the system is 54.02%, which exceeds IEEE standards.

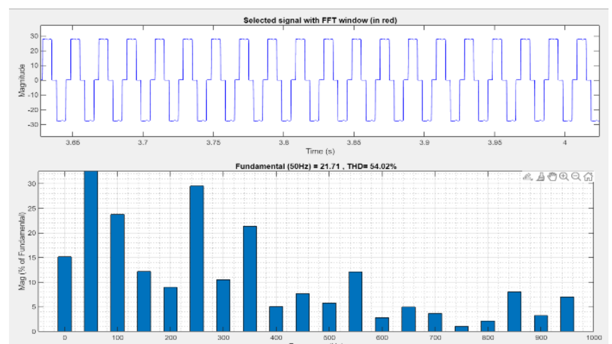

Figure 5. A diagram of the THD of the load current before compensation

With the connection of the Feed-Forward controlled SAPF into the system it was observed that the sinusoidal wave was restored to some extent and a THD of 2.58% was obtained, which is safe under the IEEE standards. With power factor increasing from 0.8673 to 0.9973.

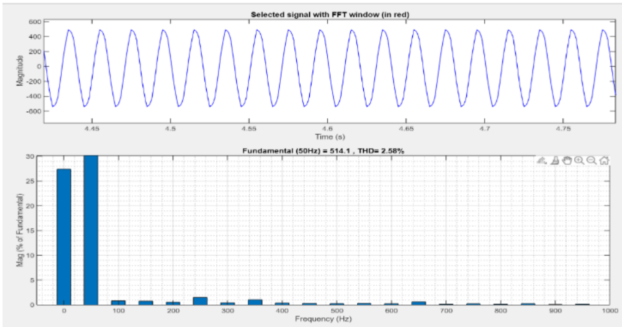

Figure 6. A diagram of the THD of the source current after compensation

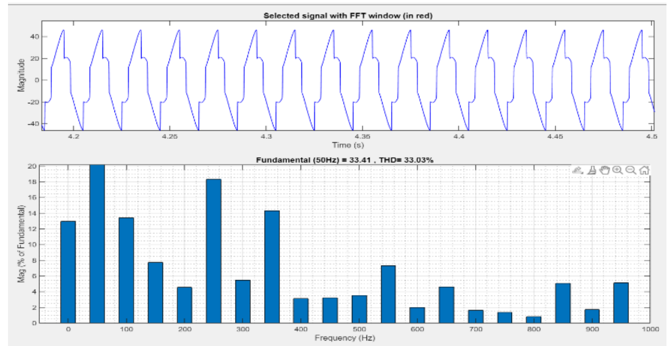

Figure 7. A diagram of the THD with added bridge impedance.

A bridge impedance of R= 10 Ω and L= 70 mH was connected to the non-linear load. The THD of the system was found to be 33.03% with a power factor of 0.4927. The THD improved to 2.49% and the power factor increased to 0.8430. Subsequent tests were performed on the system by varying the resistance which shown that the load THD varied from 53%- 60% and the source THD from 2.43%- 2.51%. The frequency of practical systems is not a constant value but varies. Due to this variation, there are standard that regulate the variations of the frequency to ensure stability in the power system. The model was tested against the allowable frequency variation that is $\pm 5\%$ of the nominal frequency. The model was tested from the range 49.5 Hz to 50.5 Hz with the results computed in a table below.

Table 2. A table of variation of THD with frequency

Frequency / Hz	Load_THD%	Source_THD%
49.50	34.56	2.79
49.70	33.79	2.56
50.10	32.65	2.51
50.30	32.27	2.51
50.50	31.51	2.57

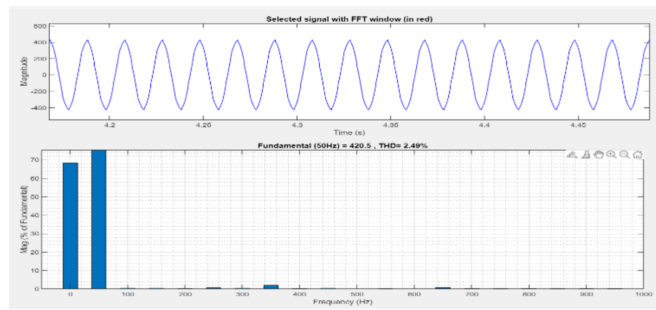

Figure 8. A diagram of the THD after compensation with added bridge impedance.

7. CONCLUSION

Feedforward Neural Network integration with shunt active power filters provide a dynamic and innovative solution to improve power quality in modern electrical systems. The project work established the implications of using Feedforward Neural Network Controlled SAPF as a potent instrument to address power quality issues, with an emphasis on its realistic application using MATLAB/SIMULINK simulation.

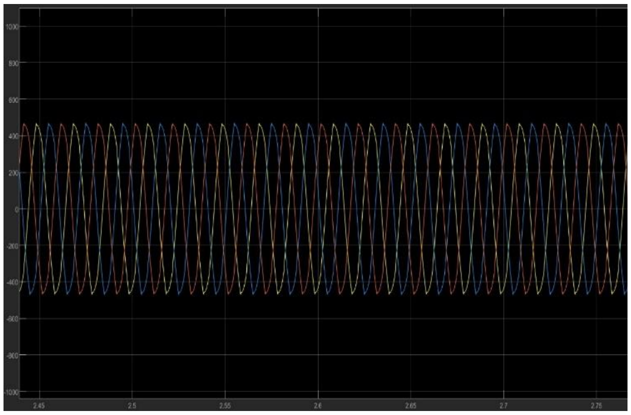

Figure 9. An illustration of the source current waveform

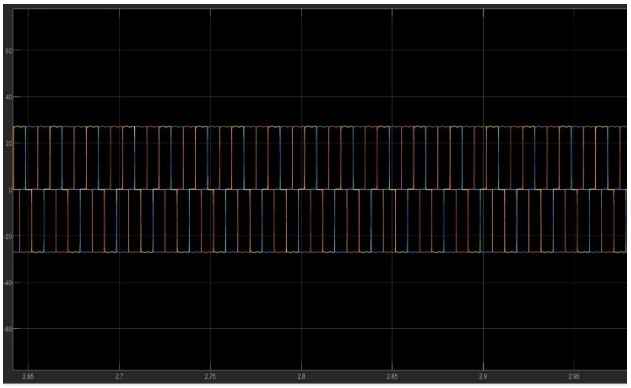

Figure 10. An illustration of the load current waveform.

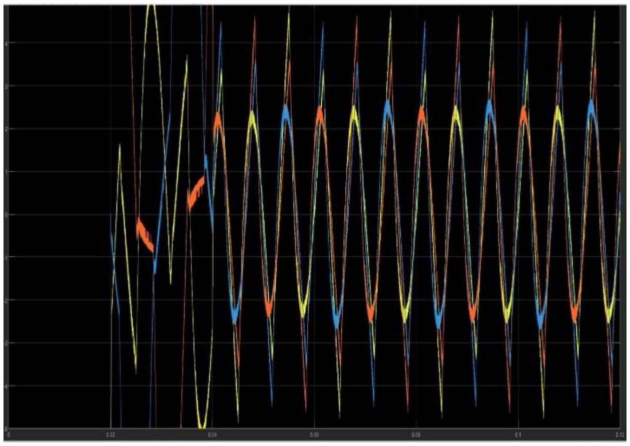

Figure 11. An illustration of the compensation current waveform

8. REFERENCE

1. P. S. a. J. A. G.-G. Juan L. Flores-Garrido, "Nonlinear Loads Compensation Using a Shunt Active Power Filter Controlled by Feedforward Neural Networks," *Applied Sciences,* vol. 11, no. 16, August 2021.

2. M. Q. a. V. Khadkikar, "Application of Artificial Neural Networks for Shunt Active Power Filter Control,," *IEEE Transactions on Industrial Informatics,* vol. 10, pp. 1765- 1774, 2014.

3. S. a. N. R. V. Jarupula, "Power Quality Improvement in Distribution System using ANN Based Shunt Active Power Filter," *International Journal of Power Electronics and Drive Systems 5,* pp. 568-575, 2015.

4. G. S. G. &. A. Joshi, " Artificial Neural Network Controlled Shunt Active Power Filter For Power Quality Improvement," *International Research Journal of Engineering and Technology (IRJET),* vol. 2, no. 4, July 2015.

5. a. V. V. Pitchumani Angayarkanni, " A Neural Network Controller with Anti Windup Based Shunt Active Power Filter for Harmonic Mitigation," 2016.

6. B. a. M. P. M. Balasubramaniam, "Implementation of Artificial Neural Network Controlled Shunt Active Power Filter for Current Harmonics Compensation," *International Journal of Advanced Research in Computer and Communication Engineering,* vol. 4, no. 5, May 2015.

7. S. M. I. C. a. R. B. Abderrahmen Benyamina, "Hybrid fuzzy logic-artificial neural network controller for shunt active power filter," *IEEE International*

Conference on Renewable Energy Research and Applications (ICRERA), pp. 837-844, 2016.

8. P. T. a. R. T. D., "Adaptive Method for Power Quality Improvement through Minimization of Harmonics Using Artificial Intelligence," *International Journal of Power Electronics and Drive Systems (IJPEDS),* vol. 8, no. 1, pp. 470 - 482, 2017.

9. A. V. S. a. M. H. G. Karan C. Patel, "Shunt active filtering with NARX feedback neural networks based reference current generation," *International Conference on Power and Embedded Drive Control (ICPEDC),* pp. 280-285, 2017.

10. N. L. a. J. Fei, "Adaptive Fractional Sliding Mode Control of Active Power Filter Based on Dual RBF Neural Networks," *IEEE Access*, vol. 5, pp. 27590-27598, November 2017.

11. S. S. D. O. A. a. J. M. L. Merabet, " Direct neural method for harmonic currents estimation using adaptive linear element.," *Electric Power Systems Research*, vol. 152, pp. 61-70, November 2017.

12. A. K. P. &. B. P. P. Prakash Chandrah Tah, "Shunt Active Filter Based on Radial Basis Function Neural Network and p-q Power Theory," *International Journal of Power Electronics and Drive Systems (IJPEDS),* vol. 8, no. 2, pp. 667-676, 2017.

13. M. A. a. D. Joshi, "Analysis of Shunt Active Filter with ANN based Controller," *International Journal of Computer Applications,* vol. 182, December 2018.

14. H. W. a. J. Fei, "Nonsingular Terminal Sliding Mode Control for Active Power Filter Using Recurrent Neural Network," *IEEE Access*, vol. 6, pp. 67819-67829, October 2018.

15. G. G. a. G. P. Kumar, "Power quality improvement at nonlinear loads using transformer-less shunt active power filter with adaptive neural fuzzy interface system supervised PID controllers," *International Transactions on Electrical Energy Systems,* vol. 30, no. 3, May 2020.

16. M. S. K. R. J. a. P. V. K.R. Sugavanam, "Convolutional Neural Network-based harmonic mitigation technique for an adaptive shunt active power filter," *Automatika*, vol. 62, pp. 471-485, October 2021.

17. A. P. a. P. K. Annu Govind, "Performance Enhancement of Shunt Active Power Filter Application using Adaptive Neural Network," *Authorea*, 24 March 2021.

18. S. F. A.-G. a. R. M. Nelms, "Performance of a Shunt Active Power Filter for Unbalanced Conditions Using Only Current Measurements," *Energies*, vol. 14, no. 2, p. 397, January 2021.

19. P. P. a. S. Wasti, "Peak Demand Management in Micro Hydro using Battery Bank," *Journal of Water, Energy and Environment,* vol. 22, no. 22, pp. 34-40, 2018.

20. S. K. I. H. a. A. M. A. Abdelhady Ramadan, "A Novel Intelligent ANFIS for the Dynamic Model of Photovoltaic Systems," *Mathematical Methods in Energy Economy*, vol. 10, no. 8, p. 1286, April 2022.

21. A. A. Imam, R. S. Kumar and Y. A. Al-Turki, "Modeling and Simulation of a PI Controlled Shunt

Active Power Filter for Power Quality Enhancement Based on P-Q Theory," *MDPI: Power Electronics,* vol. 9, no. 4, 13 April 2020.

22. R. K. a. V. Indragandhi, "Current control techniques of single phase shunt active power filter- a review," *IOP Conference Series: Materials Science and Engineering,* vol. 623, no. 1, p. 012007, October 2019.

23. S. J. K. A. Kongpan Areerak, “Harmonic Detection for Shunt Active Power Filter Using ADALINE Neural Network”, 2021.

24. M. N Uddin and M.T Amin “Design and Simulation of Active Power Filter Based on Feed Forward Neural Network for Harmonic Detection and Elimination”. 2020.

25. K. L. Areerak And T. Narongrit “Shunt Active Power Filter Design Using Genetic Algorithm Method”, 2020.

26. Hydro Ottawo “Power Quality”, 2024.

27. Michael N. D. D, Nafia Al-Mutawaly, John. L “From transmission to distribution networks-harmonic impacts on modern grid’’, 2015

28. Bhaskar. M, Ankit .S, Soumya K, James Ogle “Analyzing Distribution Transformer Degradation with Increased Power Electronic Loads”, 2021.

29. D D Reljić, Novi Sad. V. V, Vasić, Novi Sad, Serbia, Dj. V Oros, Novi Sad “Power factor correction and harmonics mitigation based on phase shifting approach”, 2021